

# The Local Group dwarf Leo T: HI on the brink of star formation

Emma V. Ryan-Weber,<sup>1\*</sup> Ayesha Begum<sup>1</sup>, Tom Oosterloo<sup>2,3</sup>, Sabyasachi Pal<sup>4</sup>,  
Michael J. Irwin<sup>1</sup>, Vasily Belokurov<sup>1</sup>, N. Wyn Evans<sup>1</sup>, and Daniel B. Zucker<sup>1</sup>

<sup>1</sup>*Institute of Astronomy, Madingley Rd, Cambridge, CB3 0HA, UK*

<sup>2</sup>*Netherlands Foundation for Research in Astronomy, Postbus 2, 7990 AA Dwingeloo, The Netherlands*

<sup>3</sup>*Kapteyn Astronomical Institute, University of Groningen, Postbus 800, 9700 AV Groningen, The Netherlands*

<sup>4</sup>*National Centre for Radio Astrophysics, Tata Institute of Fundamental Research, Pune 411-007, India*

Accepted 2007 November 15. Received 2007 November 12; in original form 2007 August 3

## ABSTRACT

We present Giant Meterwave Radio Telescope (GMRT) and Westerbork Synthesis Radio Telescope (WSRT) observations of the recently discovered Local Group dwarf galaxy, Leo T. The peak HI column density is measured to be  $7 \times 10^{20} \text{ cm}^{-2}$ , and the total HI mass is  $2.8 \times 10^5 M_{\odot}$ , based on a distance of 420 kpc. Leo T has both cold ( $\sim 500 \text{ K}$ ) and warm ( $\sim 6000 \text{ K}$ ) HI at its core, with a global velocity dispersion of  $6.9 \text{ km s}^{-1}$ , from which we derive a dynamical mass within the HI radius of  $3.3 \times 10^6 M_{\odot}$ , and a mass-to-light ratio of greater than 50. We calculate the Jeans mass from the radial profiles of the HI column density and velocity dispersion, and predict that the gas should be globally stable against star formation. This finding is inconsistent with the half light radius of Leo T, which extends to 170 pc, and indicates that local conditions must determine where star formation takes place. Leo T is not only the lowest luminosity galaxy with on-going star formation discovered to date, it is also the most dark matter dominated, gas-rich dwarf in the Local Group.

**Key words:** galaxies: dwarf – galaxies: individual (Leo T) – Local Group – galaxies: ISM – dark matter

## 1 INTRODUCTION

Leo T is an impressively small, yet complex dwarf galaxy. A member of the Local Group, Leo T is the lowest luminosity galaxy discovered to date with on-going star formation (Irwin et al. 2007). Its colour-magnitude diagram reveals both a red giant branch and young blue stars,  $\sim 6 - 8 \text{ Gyrs}$  and  $\sim 200 \text{ Myr}$  in age, respectively. Although its stellar morphology and intermediate-aged red stars are similar to the dwarf spheroidal (dSph) galaxies, many of which have been discovered recently (Belokurov et al. 2007, and references within), the presence of a younger, blue stellar population is more typical of a dwarf irregular (dIrr) galaxy. This duality has led to the ‘transition’ label, hence the name Leo T. In addition, dSph galaxies are usually found within 250 kpc of Milky Way, whereas Leo T is located at a distance of 420 kpc, similar to that of other transitional dwarfs, such as Phoenix, and dIrr galaxies (Grebel 2000). The presence of cool gas is another trademark of transitional dwarfs and dIrrs. As reported in Irwin et al. (2007), Leo T has a spatially coincident detection of HI in the Northern HI Parkes All Sky Survey (HIPASS, Wong et al. 2006). Recent optical spectroscopy has confirmed that the stellar recessional velocity matches the HI radial velocity measurement (Simon & Geha 2007).

The study of the smallest dwarf galaxies provides insight into how the least massive dark matter haloes retain cool gas and form stars. The number of dark haloes in the Local Group predicted by cosmological simulations is typically of the order of hundreds (Klypin et al. 1999; Moore et al. 1999). Only those dark haloes that can maintain sufficient cool gas, allowing star formation to proceed, produce luminous dwarf galaxies. The various processes that are thought to suppress star formation in low mass haloes include a change in the Jeans mass due to global reionization (e.g., Efstathiou 1992; Benson et al. 2002; Cooray & Cen 2005), the heating and removal of gas via supernovae and stellar wind feedback (e.g. Dekel & Woo 2003; Ricotti & Gnedin 2005), ram pressure and tidal stripping (e.g. Blitz & Robishaw 2000), or simply a temperature floor in the interstellar medium (Kaufmann et al. 2007). Mass-to-light measurements of Local Group dwarfs suggest that each galaxy is embedded in a dark matter halo with a mass of about  $10^7 M_{\odot}$  (Mateo 1998). The idea that there is a minimum dark matter halo mass able to form stars is supported by analytic calculations (Taylor & Webster 2005), observational data (Gilmore et al. 2007) and numerical simulations (Ricotti & Gnedin 2005; Read et al. 2006). Thus observations of the presence, morphology and kinematics of cool gas in dwarf galaxies provide important constraints on these predictions and hold ramifications for our understanding of galaxy formation and evolution. Leo T is a crucial piece of evidence in this line of inquiry, as it is the faintest dwarf galaxy detected to date with on-going star formation.

\* email: eryl@ast.cam.ac.uk

In this letter we present Giant Meterwave Radio Telescope (GMRT) and Westerbork Synthesis Radio Telescope (WSRT) observations that confirm the presence of H I in Leo T at higher spatial and velocity resolution than the initial detection in HIPASS. In section 3 we give the H I parameters of Leo T, and calculate the Jeans mass profile. A discussion of how star formation has proceeded in Leo T and a comparison to other Local Group dwarfs is given in section 4.

## 2 OBSERVATIONS AND DATA REDUCTION

### 2.1 GMRT data

The GMRT (Swarup et al. 1991) observations of Leo T (centred on RA (2000):  $09^h 34^m 53.5^s$ , DEC(2000):  $+17^\circ 02' 52.0''$ ) were conducted on December 12 2006. An observing bandwidth of 1 MHz centered at 1420.36 MHz (which corresponds to a heliocentric velocity of  $35 \text{ km s}^{-1}$ ) was used. The band was divided into 128 spectral channels, giving a channel spacing of  $1.65 \text{ km s}^{-1}$ . Absolute flux and bandpass calibration was done using scans on the standard calibrator 3C286, which were observed at the start and end of the observing run. Phase calibration was done using the VLA calibrator 0842+185, which was observed once every 40 minutes. The total on-source time was  $\sim 5$  hours.

The data were reduced using standard tasks in classic AIPS<sup>1</sup>. For each run, bad visibility points were edited out, after which the data were calibrated. A low resolution data cube ( $39'' \times 47''$ ) was made using the AIPS task IMAGR. The RMS noise per channel at this resolution is  $5.2 \text{ mJy beam}^{-1}$ . The H I emission from Leo T spanned 7 channels of the spectral cube. A continuum image was also made using the average of remaining line free channels. No continuum was detected at the location of Leo T to a  $3\sigma$  flux limit of  $2.3 \text{ mJy beam}^{-1}$  (for a beam size of  $39'' \times 47''$ ).

Moment maps were made from the data cube using the AIPS task MOMNT. To obtain the moment maps, lines of sight with a low signal to noise ratio were excluded by applying a cutoff at the  $2\sigma$  level ( $\sigma$  being the rms noise level in a line free channel), after smoothing in velocity (using boxcar smoothing three channels wide) and position (using a Gaussian with a FWHM approximately twice that of the synthesized beam). A map of the velocity dispersion was also made in GIPSY<sup>2</sup> using single Gaussian fits to the individual profiles. From the Gaussian fits, we find a median velocity dispersion  $\sigma_v \sim 3 \text{ km s}^{-1}$ .

### 2.2 WSRT data

Leo T was observed with the WSRT on the night of February 16/17, 2007. The observations consisted of a full 12-hr synthesis, using the so-called maxi-short configuration that gives good coverage of the inner  $uv$  plane, although, given the low declination of Leo T, data collected at extreme hour angles had to be flagged because of shadowing on the shortest baselines. The observing bandwidth was 5 MHz (corresponding to about  $1000 \text{ km s}^{-1}$ ), using 1024 channels with 2 independent polarisations. The data processing was done using the MIRIAD package (Sault et al. 1995). Before and after the 12-hr observation, a standard WSRT calibrator was observed

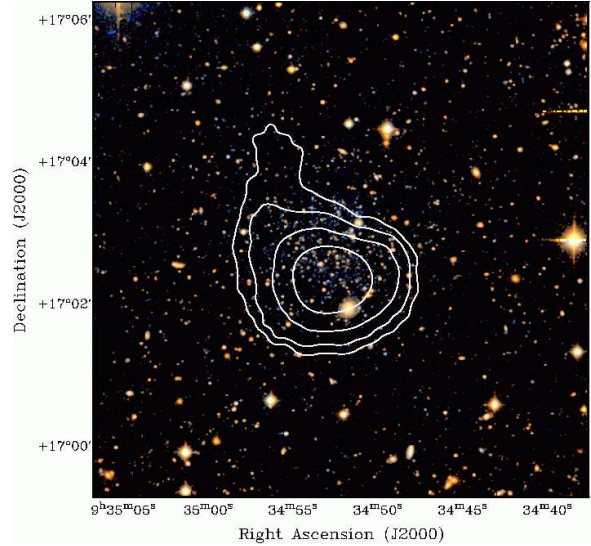


**Figure 1.** Colour image of Leo T from INT WFC  $g$  and  $r$  band data with GMRT H I contours overlaid. The column density contours at  $2, 5, 10$  and  $20 \times 10^{19} \text{ cm}^{-2}$ , and the beam size is  $39'' \times 47''$ .

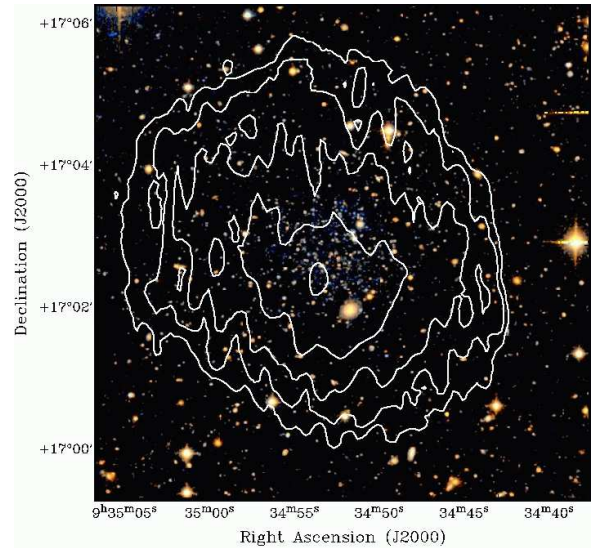


**Figure 2.** The same colour image from Figure 1, however the H I contours are from the WSRT data. In this case, the column density contours  $2, 5, 10, 20$  and  $50 \times 10^{19} \text{ cm}^{-2}$ , and the beam size is  $12.9'' \times 50.4''$ . An explanation for the difference between the GMRT and WSRT detections is given in Section 3.

(3C147 and CTD93), from which the spectral response of the telescope was determined. As is standard practice with the WSRT, during the 12-hr track no additional (phase) calibrators were observed. Instead, the large bandwidth allows us to determine the gain variations by self-calibration of the continuum image made from the line-free channels of the data.

Two datacubes were made, with spatial resolutions  $12.9'' \times 50.4''$  and  $28.2'' \times 45.2''$ , respectively. Each datacube was gridded into 900 channels  $1.0 \text{ km s}^{-1}$  wide to which additional Hanning

<sup>1</sup> Astronomical Image Processing System

<sup>2</sup> Groningen Image Processing SYstem

**Table 1.** Measured and derived properties of Leo T from H I data

Parameter	
Optical coordinates (J2000)	09:34:53.4 +17:03:05
H I centre	09:34:53.5 +17:02:22
H I radius, $r_{\text{HI}}$	2.5' (300 pc)
$S_{\text{int}}$	6.7 Jy km s <sup>-1</sup>
$M_{\text{HI}}$	$2.8 \times 10^5 M_{\odot}$
$N_{\text{HI}}(\text{peak})$	$7 \times 10^{20} \text{ cm}^{-2}$
$v_{\odot}$	38.6 km s <sup>-1</sup>
$\sigma_v(\text{CNM } T \sim 500 \text{ K})$	2 km s <sup>-1</sup>
$\sigma_v(\text{WNM } T \sim 6000 \text{ K})$	7 km s <sup>-1</sup>
$\sigma_v(\text{global profile})$	6.9 km s <sup>-1</sup>
$M_{\text{dyn}}$	$> 3.3 \times 10^6 M_{\odot}$
$r_{\text{HI}}/r_{\text{Plummer}}$	1.8
$M_{\text{dyn}}/L_V$	$> 56$
$f_{\text{gas}} = M_{\text{gas}}/(M_{\text{gas}} + M_{\text{star}})$	0.8
$f_{\text{baryonic}} = (M_{\text{gas}} + M_{\text{star}})/M_{\text{dyn}}$	0.15

smoothing was applied, for a resulting velocity resolution of 2.0 km s<sup>-1</sup>. The datacubes were cleaned using the Clark (1980) algorithm. In an iterative procedure, regions with line emission were identified by smoothing the data to twice the spatial resolution and selecting a clip level by eye to define the masked region where the data were cleaned. This procedure was repeated until convergence was achieved. The final noise in the Hanning-smoothed data is 1.3 and 2.0 mJy/beam for the high and low resolution datacubes respectively.

To construct the total H I images and the velocity fields, the same masks were used. The H I flux integral is 6.7 Jy km s<sup>-1</sup>, corresponding to a H I mass of  $2.8 \times 10^5 M_{\odot}$  (using a distance to Leo T of 420 kpc). The mass derived here – given the uncertainties of the original detection – is consistent with that derived from the HIPASS data ( $2 \times 10^5 M_{\odot}$ ). No continuum source associated with Leo T was detected to a  $3\sigma$  flux limit of 0.5 mJy beam<sup>-1</sup>.

### 3 HI PROPERTIES

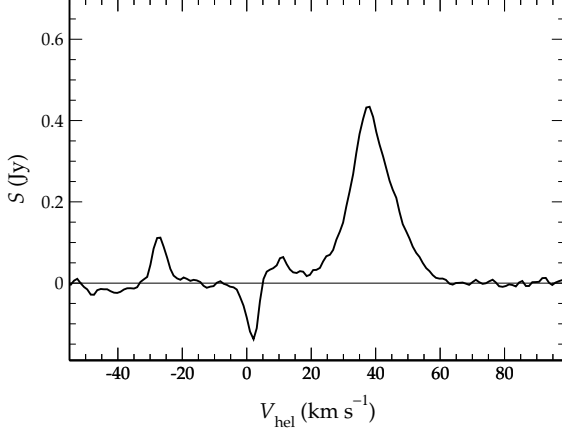
The GMRT observations detect a central, cool core of H I (see Figure 1), as evidenced from the low median velocity dispersion of 3 km s<sup>-1</sup>. The mass of H I contained in this cool component is  $1.2 \times 10^5 M_{\odot}$ , which is approximately 40 per cent of the total H I mass of Leo T. At the resolution of the images presented in Figures 1 and 2 there is a factor of four difference in sensitivity. Formally the GMRT data have a 1 channel  $3\sigma$  column density sensitivity of  $2 \times 10^{19} \text{ cm}^{-2}$ . Comparing the contours in Figures 1 and 2 it is obvious that despite the formal sensitivity, the GMRT observations miss a substantial fraction of the flux in the outer parts of Leo T. Due to GMRT's lack of short baselines, the GMRT observations fail to detect the warmer component of the H I, which is spread over a larger spatial scale. The WSRT data detect H I out to a radius of 2.5', or 300 pc (using a distance of 420 kpc). We are confident that this is the true extent of H I in Leo T, as the entire HIPASS flux density is recovered by the WSRT observations. The centre of the H I detection is 40'' to the south of the stellar centre of Leo T. This offset is less than the extent of the beam major axis for both the GMRT and WSRT observations, although it is interesting to note that the same offset is found in the two independent data sets.

Figure 3 shows the global H I profile from the WSRT data. The global kinematic properties of the H I are in good agreement

with the stars, which have a mean velocity of 38.1 km s<sup>-1</sup> and a velocity dispersion of 7.5 km s<sup>-1</sup> (Simon & Geha 2007). Leo T has a chaotic velocity field, with some evidence of a gradient, but no indication of systematic rotation (see Figure 4). This type of velocity field is typical of the H I in low mass dIrr galaxies that have been observed with sufficient velocity resolution, for example, LSG-3 (Young & Lo 1997). Interestingly, recent results from FIGGS (Faint Irregular Galaxies GMRT Survey) have now shown that most dwarf galaxies below a dynamical mass of  $\sim 10^8 M_{\odot}$ , show velocity fields that are either completely chaotic or show large scale patterns that are not consistent with systematic rotation (Begum et al., in preparation). We measure a global H I velocity dispersion of 6.9 km s<sup>-1</sup>, although the GMRT data indicate that there is a central component of cold gas with a much lower dispersion. Figure 5 gives the velocity dispersion histogram across the whole face of Leo T using the WSRT data, where a single Gaussian is fit to each pixel in the data cube, and the  $\sigma_v$  recorded. A second histogram shows the results of a double Gaussian fit to each pixel in the bright, central region of Leo T. The double Gaussian describes the shape of the spectra substantially better in the central region, as evidenced from the significant residuals that result from fitting a single Gaussian. The double Gaussian fits show that gas in the centre of Leo T consists of cold (2 km s<sup>-1</sup>,  $T \sim 500\text{K}$ ) and warm (7 km/s,  $T \sim 6000\text{K}$ ) components. This two-phased medium is typical of faint dIrr galaxies; double-Gaussian line profile fits of a sample of ten gas-rich dwarf galaxies (Begum et al. 2006) show narrow components of the velocity dispersion in the range 2 – 7 km s<sup>-1</sup>, while broad components range in value from 6 to 17 km s<sup>-1</sup>. Some Local Group galaxies also exhibit a similar two-phased interstellar medium, for example, Leo A (Young & Lo 1996) and Sag DIG (Young & Lo 1997). By contrast the Local Group dwarf LGS 3 - which has ceased forming stars - lacks a cold H I phase (Young & Lo 1997). In Leo T, the single Gaussian fit pixels in all regions give velocity dispersions ranging from 3 to 15 km s<sup>-1</sup>, with a median of 7.8 km s<sup>-1</sup>. The high dispersion tail (11 – 15 km s<sup>-1</sup>) corresponds to a region 30'' North and 70'' East of the H I centre.

Given the lack of any systematic rotation, it is difficult to accurately determine the total dynamical mass for Leo T. Assuming the system is in equilibrium and that the H I dynamics are a fair tracer of the overall mass distribution the virial theorem can be used to determine the mass. Applying the virial theorem under the assumption of a spherical H I distribution and an isotropic velocity dispersion with negligible rotation, the dynamical mass is given by  $M_{\text{dyn}} = r_g \sigma_v^2 / G$ , where  $r_g$  is the gravitational radius,  $\gtrsim 300$  pc, and  $\sigma_v = 6.9$  km s<sup>-1</sup> from the global profile. Thus, the total dynamical mass is  $M_{\text{dyn}} \gtrsim 3.3 \times 10^6 M_{\odot}$ . This is a lower limit to the total mass, as the dark matter may be more extended than the H I. Simon & Geha (2007) estimate a total mass of  $7.3 \times 10^6 M_{\odot}$ , using the stellar velocity dispersion and a method that accounts for a more extended gravitational radius based on the Plummer profile. Leo T is quite gas rich, with more mass contained in H I than in stars. Specifically, given its luminosity  $L_V = 6 \times 10^4 M_{\odot}$ , then assuming a conservative stellar mass-to-light ratio of 2, we obtain a stellar mass of  $M_{\text{star}} \sim 1.2 \times 10^5 M_{\odot}$ . If we correct for Helium and metals (but not molecular gas) the gas fraction of Leo T is 80 per cent. Given the extremely low stellar mass, the observed mass-to-light of Leo T is quite high,  $M_{\text{dyn}}/L_V \gtrsim 56$ .

To explore the relationship between the H I properties and the location of stars in Leo T we calculate the differential Jeans mass profile. For a spherically symmetric system, with uniform density



**Figure 3.** The global H I spectrum of Leo T from the WSRT data in the heliocentric frame. Emission at less than 20 km s<sup>-1</sup> does not appear to be physically connected to Leo T. The negative feature is poorly imaged Galactic H I due to the lack of short baselines.

$\langle \rho \rangle$ , the Jeans mass is given by

$$M_{\text{Jeans}} = \frac{1}{6} \pi \langle \rho \rangle \left( \frac{\pi c_s^2}{G \langle \rho \rangle} \right)^{3/2} \quad (1)$$

(Eqn 5-24, Binney & Tremaine 1987). In a gaseous system, the sound speed  $c_s$  is related to the velocity dispersion,  $\sigma_v$ , by  $c_s = \sigma_v / \sqrt{5/3}$  (e.g. Schaye 2004). The assumption of homogeneity in Equation 1 only affects the timescale of the collapse, not the stability condition itself (Penston 1969). Thus, we can use the measured density and velocity dispersion profiles to calculate the cumulative Jean mass. The H I column density is related to the three dimensional density  $\rho$  by

$$\rho(r) = -\frac{m_p}{\pi} \int_r^\infty \frac{dN_{\text{HI}}}{dR} \frac{dR}{\sqrt{R^2 - r^2}} \quad (2)$$

(Eqn 4-58, Binney & Tremaine 1987). The radially averaged velocity dispersion smooths over the features seen in Figure 5, although a radial trend still exists, with a mean  $\sigma_v$  of 3.5 km s<sup>-1</sup> in the centre, increasing to 7 km s<sup>-1</sup> at 230 pc. The velocity dispersion profile is only calculated to a radius of 230 pc, as noise in the data leads to a number of unreliable  $\sigma_v$  measurements in individual pixels in the outskirts of Leo T. Therefore we have only calculated the Jeans mass to this radius. The falling H I column density and increasing mean velocity dispersion cause the differential Jeans mass to increase with radius, as shown in Figure 6. The dynamical mass enclosed at radius  $r$ ,  $M_{\text{dyn}}(r)$ , does not exceed the Jeans mass at any radius.

#### 4 STAR FORMATION IN A LOW MASS HALO

Given its stellar mass of  $\sim 1.2 \times 10^5 M_\odot$  and age of  $\sim 6 - 8$  Gyrs, on average, Leo T has been forming stars at the slow rate of  $1.5 - 2 \times 10^{-5} M_\odot$  per year. Evidently this gentle star formation rate has neither heated nor blown out all the gas in Leo T, allowing the stellar mass to build. A reservoir of approximately  $10^5 M_\odot$  of cool gas ( $\sigma_v = 2$  km s<sup>-1</sup>,  $T \sim 500$  K) remains, which would take about  $5 \times 10^9$  years to exhaust at the average past star formation rate. Since Leo T appears to be on such a gentle trajectory with respect to the Galactic Standard of Rest ( $-58$  km s<sup>-1</sup>) and Local Group ( $-97$  km s<sup>-1</sup>), it is possible that its gas has avoided being

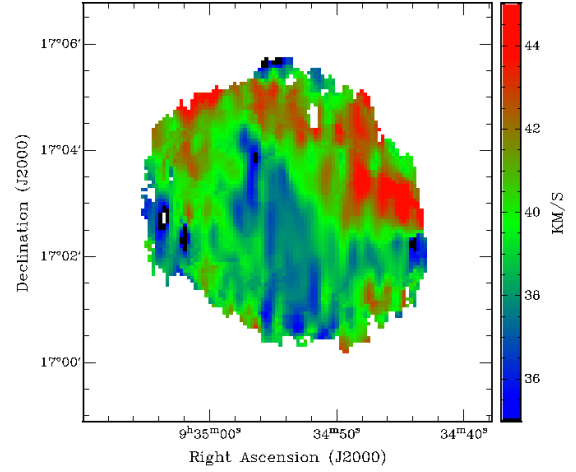


**Figure 4.** The velocity field of Leo T derived from WSRT data; the field is chaotic, with little evidence for rotation.

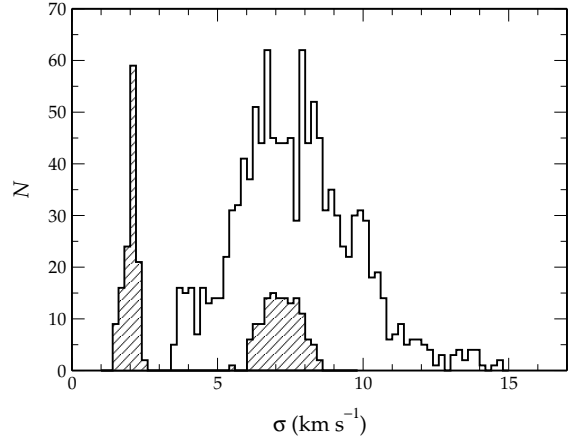


**Figure 5.** Histogram of H I velocity dispersions from the WSRT data. The unshaded histogram gives the distribution of  $\sigma_v$  values from fitting a single Gaussian to the velocity profile at each spatial pixel in the data cube. In the central bright region, these fits have significant systematic residuals, thus double Gaussian fits to pixels in this region are warranted. The shaded histogram gives the distribution of  $\sigma_v$  values for a double Gaussian fit to velocity profiles in the bright central region.

stripped or heated by an interaction. Such a low central velocity dispersion ( $\sigma_v = 2$  km s<sup>-1</sup>) may be the reason why this galaxy has been able to form stars despite its peak H I column density ( $7 \times 10^{20}$  cm<sup>-2</sup>) being lower than those of typical low surface brightness dwarf galaxies (van Zee et al. 1997).

The Plummer law fit gives a stellar radius of  $1.4'$  (Irwin et al. 2007), corresponding to a physical length of 170 pc. An excess of stars above the background is detected out to a radius of  $5'$ . Visual inspection of the image in Figures 1 and 2 shows that the over density of blue stars lies within  $1'$ , or 120 pc of the centre. The Jeans mass analysis suggests that the gas is stable against collapse, contrary to what is observed. This prediction is based the assumption of a spherical distribution and radially averaged H I column density and velocity dispersion. Flattening the density distribution causes the Jeans mass decrease. Since Leo T appears to be stable against star formation globally, it must be local processes that

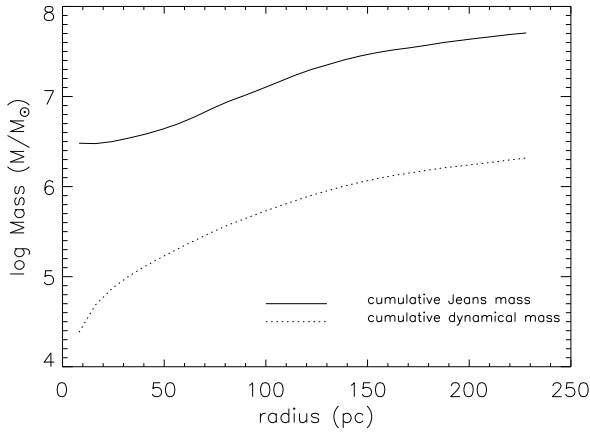


**Figure 6.** Cumulative Jeans mass (solid line) and dynamical mass profile (dotted line) of Leo T. The Jeans mass profile is derived from the radially averaged column density and velocity dispersion (see Equation 1 and 2).

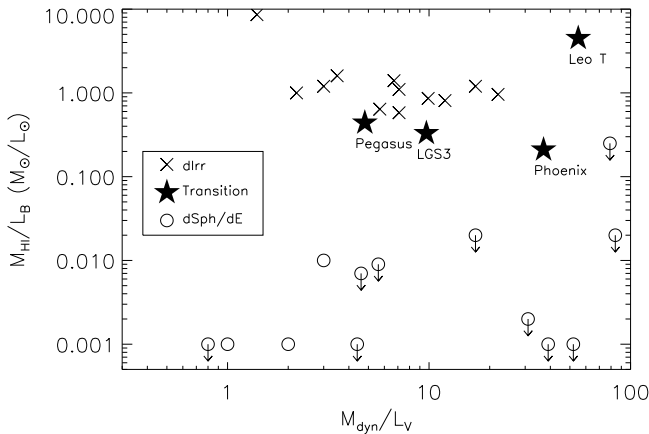


**Figure 7.** Comparison of mass-to-light properties of Leo T with Local Group dwarf galaxies, where both the dynamical mass and at least a limit on the H I is known. The  $M_{\text{HI}}/L_B$  and total mass-to-light ratios are taken from Mateo (1998), Table 4. Arrows indicate upper limits to the H I mass measurements.

govern the star formation. The tendency for locations with narrow velocity components to coincide with H I column densities above  $3 \times 10^{20} \text{ cm}^{-2}$  supports this idea. Furthermore, a small level of star formation may increase the turbulence, inhibiting the global collapse, but promoting local instabilities via density fluctuations (Schaye 2004).

It would be interesting to repeat the radial Jeans mass analysis on compact high velocity clouds (HVCs) to see whether their H I properties suggest that star formation is possible. The analysis would be straightforward since column density and velocity dispersion measurement are independent of distance, an issue that has plagued the interpretation of HVCs. Although Leo T is more compact than any of the compact HVCs for which high resolution imaging is available (Braun & Burton 2000), their peak column densities ( $\sim 4 \times 10^{20} \text{ cm}^{-2}$ ) and minimum velocity dispersions ( $< 1 \text{ km s}^{-1}$ ) are similar to those of Leo T. The initial detection of an H I cloud at the location of Leo T in the HIPASS data was indistinguishable from an HVC. It is only the high resolution H I imaging presented here, together with a recessional velocity measurement of the stars in Leo T that has lead to the confirmation that the H I

detected is of Leo T itself. Given the similarity in H I characteristics, it is quite possible that compact HVCs represent a population of ‘failed’ galaxies that contain gas and no stars, with masses akin to that of Leo T. Confirming this suggestion, however, will be quite difficult, as distance measurements rely on the chance alignment with both a foreground and background object, and the sky area covered by compact HVCs is small.

Compared with other dwarf galaxies in the Local Group, Leo T contains a significant component of dark matter given its large gas fraction. In Figure 7, dIrr galaxies tend to populate the top left of the diagram, characterized by high gas fractions ( $M_{\text{HI}}/L_B > 0.1$ ) and typical total mass-to-light ratios less than 10. On the other hand, the lower half of the diagram is occupied by dSph galaxies, which have low gas fractions (mostly upper limits as no H I is detected in many cases) and total mass-to-light ratios ranging from 1 to 100. The three other galaxies classified as transitional dwarfs have properties that lie in between the dIrr and dSph galaxies in Figure 7. Leo T appears to stand alone in the top right of diagram, it is significantly more gas rich and also contains more dark matter than other transitional dwarfs.

The number and nature of Local Group dwarf galaxies provide important constraints on models of galaxy formation and evolution. How many other extremely low-luminosity, gas-rich galaxies are yet to be found in the Local Group? The SDSS (Sloan Digital Sky Survey) has surveyed one fifth of the sky, and has uncovered just one such gas-rich dwarf, namely Leo T. The completeness for similar objects over the SDSS survey area is close to one (Koposov et al. 2007), thus only a handful of other discoveries of comparable luminosity are expected in other directions, assuming an isotropic distribution. The other avenue to explore is detection via the H I emission line. Compared with HIPASS, current surveys, such as the Arecibo Galactic H I Survey (Stanimirovic et al. 2006) will provide four-times better spatial resolution with  $0.2 \text{ km s}^{-1}$  velocity resolution, and the Galactic All Sky Survey (GASS, McClure-Griffiths et al. 2006) will provide a 20-fold improvement in velocity resolution. Disentangling extragalactic H I (with a chaotic velocity field) from emission associated with the Galaxy at low Galactocentric velocities will always remain an issue; the only definitive test is a matching velocity for the stellar component of the object.

## 5 SUMMARY

We have confirmed the presence of  $2.8 \times 10^5 M_\odot$  of H I in the Local Group dwarf galaxy, Leo T. The gas is essentially centred on the stellar emission with a radial extent of 300 pc. The H I consists of both a cold and warm neutral medium, revealed by a double Gaussian fit with  $\sigma_v = 2, 7 \text{ km s}^{-1}$  to pixels in the central region; the velocity dispersion of the global profile is  $6.9 \text{ km s}^{-1}$ . The comparatively low stellar mass gives Leo T a high gas fraction of 80 per cent. The H I extent and velocity dispersion of gas have been used to estimate a total dynamical mass for Leo T,  $M_{\text{dynamical}} \gtrsim 3.3 \times 10^6 M_\odot$ . This value for the total mass is just lower than the fiducial  $10^7 M_\odot$ , below which galaxies are expected to be dark (e.g., Read et al. 2006), due to supernova feedback and reionization. Although the simulations predict that most gas-rich dwarf galaxies form in haloes with  $M > 10^8 M_\odot$ , there are some rare examples of galaxies in simulations that have a dark matter halo mass of  $\sim 10^7 M_\odot$  and a small baryon fraction that do form at least some stars, albeit inefficiently (Ricotti & Gnedin 2005) – a description which fits Leo T. It is interesting to note that Leo T has a significant fraction of dark matter; given that most gas-rich

dwarfs (i.e. dIrr) have  $M_{\text{dyn}}/L_V$  values between 1 and 10, the total mass of Leo T would be expected to be about  $10^5 M_\odot$ , yet a mass in excess of  $10^6 M_\odot$  has been measured, thus upholding the idea of a minimum dark matter halo mass for dwarf galaxies (Mateo 1998; Gilmore et al. 2007). We have compared the cumulative dynamical and Jeans masses to determine that the H I in Leo T is *globally* stable against star formation, this is inconsistent with the observed presence of young stars. From this we conclude that local rather than global processes must be responsible for Leo T's stellar component. The very low past average star formation rate may be the reason why such cold gas is able to reside in Leo T.

## ACKNOWLEDGMENTS

The observations at the GMRT were conducted as a part of Director's Discretionary time. The GMRT is operated by the National Center for Radio Astrophysics of the Tata Institute of Fundamental Research. The WSRT is operated by the Netherlands Foundation for Research in Astronomy (ASTRON) with the support from the Netherlands Foundation for Scientific Research (NWO).

## REFERENCES

- Begum A., Chengalur J. N., Karachentsev I. D., Kaisin S. S., Sharina M. E., 2006, MNRAS, 365, 1220
- Belokurov V., et al. 2007, ApJ, 654, 897
- Benson A. J., Frenk C. S., Lacey C. G., Baugh C. M., Cole S., 2002, MNRAS, 333, 177
- Binney J., Tremaine S., 1987, Galactic dynamics. Princeton, NJ, Princeton University Press, 1987, 747 p.
- Blitz L., Robishaw T., 2000, ApJ, 541, 675
- Braun R., Burton W. B., 2000, A&A, 354, 853
- Clark B. G., 1980, A&A, 89, 377
- Cooray A., Cen R., 2005, ApJ, 633, L69
- Dekel A., Woo J., 2003, MNRAS, 344, 1131
- Efstathiou G., 1992, MNRAS, 256, 43
- Gilmore G., Wilkinson M. I., Wyse R. F. G., Kleya J. T., Koch A., Evans N. W., Grebel E. K., 2007, ApJ, 663, 948
- Grebel E. K., 2000, in Favata F., Kaas A., Wilson A., eds, ESA SP-445: Star Formation from the Small to the Large Scale The Star Formation History of the Local Group. p. 87
- Irwin M. J., et al. 2007, ApJ, 656, L13
- Kaufmann T., Wheeler C., Bullock J. S., 2007, MNRAS, submitted, astro-ph/0706.0201
- Klypin A., Kravtsov A. V., Valenzuela O., Prada F., 1999, ApJ, 522, 82
- Koposov, S. et al. 2007, ApJ, submitted, astro-ph/0706.2687
- Mateo M. L., 1998, ARA&A, 36, 435
- McClure-Griffiths N. M., Ford A., Pisano D. J., Gibson B. K., Staveley-Smith L., Calabretta M. R., Dedes L., Kalberla P. M. W., 2006, ApJ, 638, 196
- Moore B., Ghigna S., Governato F., Lake G., Quinn T., Stadel J., Tozzi P., 1999, ApJ, 524, L19
- Penston M. V., 1969, MNRAS, 144, 425
- Read J. I., Pontzen A. P., Viel M., 2006, MNRAS, 371, 885
- Ricotti M., Gnedin N. Y., 2005, ApJ, 629, 259
- Sault R. J., Teuben P. J., Wright M. C. H., 1995, in Shaw R. A., Payne H. E., Hayes J. J. E., eds, ASP Conf. Ser. 77: Astronomical Data Analysis Software and Systems IV A Retrospective View of MIRIAD. p. 433
- Schaye J., 2004, ApJ, 609, 667
- Simon J. D., Geha M., 2007, ApJ, submitted, astro-ph/0706.0516
- Stanimirović, S. et al. 2006, ApJ, 653, 1210
- Swarup G., Ananthakrishnan S., Kapahi V. K., Rao A. P., Subrahmanya C. R., Kulkarni V. K., 1991, Current Science, 60, 95
- Taylor E. N., Webster R. L., 2005, ApJ, 634, 1067
- van Zee L., Haynes M. P., Salzer J. J., Broeils A. H., 1997, AJ, 113, 1618
- Wong O. I., et al. 2006, MNRAS, 371, 1855
- Young L. M., Lo K. Y., 1996, ApJ, 462, 203
- Young L. M., Lo K. Y., 1997, ApJ, 490, 710

This paper has been typeset from a  $\text{\LaTeX}$  file prepared by the author.